Original Research Article

J. Funct. Mater. Biomol. 2(2)-2018 pp 53-57

SACRED HEART RESEARCH PUBLICATIONS

Journal of Functional Materials and Biomolecules

Journal homepage: www.shcpub.edu.in

ISSN: 2456-9429

Investigation on the effect of Lanthanum substituted copper oxide nanoparticles synthesized by co-precipitation method

John.D.Rodney[1], S. Deepapriya[1], P. Annie Vinosha[1], S. Jerome Das[1]*

Received on 26 Nov 2018, Accepted on 31 Dec 2018

Abstract

Binary nano metal oxides are extensively pursued for their prominence in various fields of technological application for the development of nano structured materials to enrich their retail properties. Admits these transitional metal oxides, Copper oxide is determined to be a potential candidate due to its versatile structural, optical and thermal properties. The rare earth element, lanthanum was used as a dopant because of their tendency to boost the optical and thermal properties and tune the material in a desired way. Here the lanthanum doped and undopedCuO nanoparticles were synthesized using a swift and elegant co-precipitation synthesis. The crystallite size and the structural parameters was determined using the X-Ray diffraction spectra, the fingerprint vibrational modes were confirmed using the FT-IR spectra for a range of 4000 – 500 cm^{-1}, the optical band gap for the material was understood from the UV-vis spectra for a range of 300–700 nm and the microstructural nature of the material was studied from the raman spectra from a range of 200–1350cm^{-1}. The morphological characteristics of the given material was seen using the TEM micrograph. The overall result of the effect of lanthanum on copper oxide were studied.

Keywords: copper oxide, co-precipitation, optical property.

1 Introduction

Nanomaterials are enticing more prominence nowadays because of their efficacy in our per diem applications, out of which the metal oxides nanoparticles have brought in ponderous attention in research due to their multivarient properties in different field of applications [1]–[3]. Amidst these d-block elements CuO has proven to be a standalone because of its inimitable prospects. The CuO nanoparticles are far and wide pursued by the researchingcommunity because of their peculiar properties when correlated with their bulk [4]. The CuO nanoparticle is a potential p-type semiconductor with a narrow bandgap of 1.2 eV [5]. The assets of CuO nanoparticles chiefly depends upon structure, composite, size and shape of the nanocrystals. Thus stimulating phenomenon such as higher surface to volume ratio, quantum confinement effect and significant change in surface energy can be obtained when the metal oxides is reduced to nanoscale dimension. Ample types of synthesis are implied to obtain CuO nanoparticles with different size, morphology and properties [6] and here we have commenced a instantaneous and cost effective co-precipitation method [7]. The Pure CuO nanoparticles and 2% La doped CuO nanoparticles are synthesized and the outcome of doping La ions in CuO nanoparticles is briefly studied.

2 Experimental

2.1 Chemicals

The AR graded Merck chemicals, copper (II) nitrate trihydrate $Cu(NO_3)_2.3H_2O$, sodium hydroxide pellets NaOH and lanthanum nitrate hexahydrate $La(NO_3)_3.6H_2O$ were used without any further purification for the synthesis of lanthanum doped copper oxide nanoparticles.

2.2 Synthesis of CuO Nanoparticles

Pure CuO and 2% La doped CuO nanoparticles were synthesized by a standardized chemical precipitation method (fig.1). A homogeneous aqueous solution of copper (II) nitrate trihydrate and lanthanum nitratehexahydrate was formed by measuring them to their stoichiometric ratio and adding them with 50ml of double distilled water and stirred together for 1 hour in a reaction glass vessel, followed by the addition of 2M NaOH onto the aqueous solution as a precipitator. The pH of the solution was maintained at 14. The subsequent solution was heated at 70°C for 3 hours with uninterrupted stirring and then it was cooled down to room temperature[8]. The blackish precipitate was centrifuged twice with double distilled water followed by twice with ethanol in order to separate nitrates and other impurities existing in it. The precipitate was dried overnight at 60°C in hot air oven and then stupendously grounded to powder. The grounded sample was then calcined in muffle furnace at 350°C for 3 hours and the consequential product was scrutinized for its structural, morphological and optical properties.

* Corresponding author e-mail: jeromedas.s@gmail.com, jerome@loyolacollege.edu, Phone: +91-9094139314

[1] Department of Physics, Loyola College, Chennai, 600 034, India

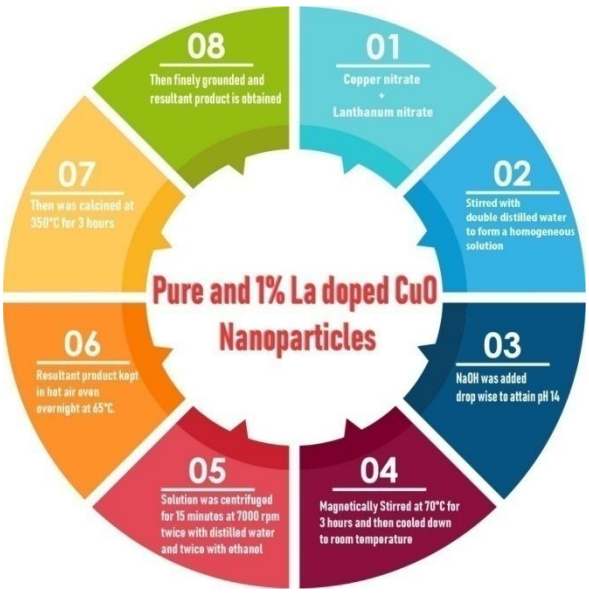

FIGURE 1: A schematic representation of synthesis procedure for pure and 1% La doped CuO nanoparticles

2.3 Characterization

Structural studies of these samples were conceded out by BrukerD8 advance powder X-ray diffractometer in the 2θ range of 20°-80° in steps of 0.017° using $CuK\alpha_1$ radiation (1.54056Å). The XRD patterns were related with standard JCPDS card number 89-5895 for CuO nanoparticle from the ICDD database and the structural parameters were confirmed. The FTIR absorption behavior of the assynthesized samples was acquired using Perkin-Elmer Spectrum FTIR spectrometer with a scanning range of 4000 – 400 cm^{-1}. The Agilent Carey 5000 UV Visible spectrophotometer made in United States was used to determine the optical property of the given samples for a range of 200- 800 nm. The Raman spectroscopy was determined by Renishaw InVia Raman microscope made in United Kingdom for a range of 200 to 1350 cm^{-1} and the morphology of the nanoparticles was examined using Joel/JEM 2100 Transition Electron Microscope.

3 Results and Discussion

3.1 Structural analysis: X-ray diffraction

The unique XRD pattern for pure CuO and 2% lanthanum doped CuO nanoparticles is as shown in the fig.2. The XRD patterns is compared with the JCPDS card no (89-5895) [9]and correlating the peak positions it is understood that the monoclinic structure of CuO is retained even after doping of La^{3+} ions.In addition no further impurity peaks where detected in the pattern, this implies that the nanoparticles retain its metal oxide status and is seen that as the La^{3+}dopant is added the peak becomes broader and increases in, this change in the crystallite size was calculated using Scherrer's formula [10].

$$D = \frac{0.9\,\lambda}{\beta \cos\theta} \qquad (1)$$

where λ is the wavelength of X-ray radiation (1.5406Å), β is the full width at half maximum (FWHM) of the peaks at the diffracting angle θ[11]. Using Gaussian convoluting profile the β can be obtained from FWHM. The broadening β_r is [8],

$$\beta_r^2 = \beta_0^2 - \beta_i^2 \qquad (2)$$

Where β_i is the instrumental broadening and β_0 is observed broadening. The average crystallite size for undoped and 2% La doped CuO and the change in the lattice parameters are listed down in table.1.

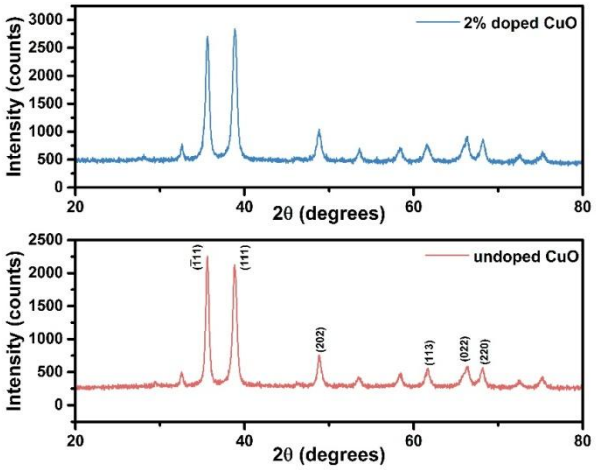

FIGURE 2. XRD pattern of Pure CuO& 2% La doped CuO NPs

Table.1 Estimated lattice parameters and crystallite size

Samples	a (Å)	b (Å)	c (Å)	D(nm)
Pure CuO	4.7250	3.4166	5.0588	15
CuO + 2% La	4.7187	3.4141	5.0731	14

From the above table, it's clinched that there is a slight decrease in the crystallite size as the dopant is added and the La doped CuOXRD peaks tend to be wider when compared to the pure CuO. This phenomenon of decreased crystallite size suggests the impact of the grain boundary restriction effect of the rare earth onto the host material and it is clearly seen that as the dopant is added the nanoparticles overcomes the conventional quantum confinement effect and exhibits the pressure induced effect during the incorporation of La^{3+} ions onto the host lattice sites thus in turn reduces the crystallite size by a margin.

3.2 FTIR Analysis

The FTIR spectra of pure and lanthanum doped CuO nanoparticles were logged at room temperature for a range of 4000-400 cm^{-1} [12]. Fig.3, shows palpable transmittance bands at 504 cm^{-1} and 427 cm^{-1} for pure CuO and 442 cm^{-1} for lanthanum doped CuO NP's whichwere allotted to the vibrational mode of Cu(II)-O

bands. The absorption band at 1516 cm^{-1}, 1382 $cm^{-1}$for pure CuO and 1321 $cm^{-1}$and 1412 $cm^{-1}$for La^{3+} doped CuO NP's is due to the stretching vibration of C=O bond. The absorption band at 3739 cm-1 for pure CuO and 3728 cm^{-1} for lanthanum doped CuO is due to the stretching vibration of captivated H-O-H bonding of absorbed water [13], [14] and the minor peak at 2360 cm^{-1} is due to the residue C-H bond vibration present in it due to the ambient effect [15]. The shift in transmittance band from 427 to 442 cm^{-1} indicates that there is a complexation of copper oxide and lanthanum.

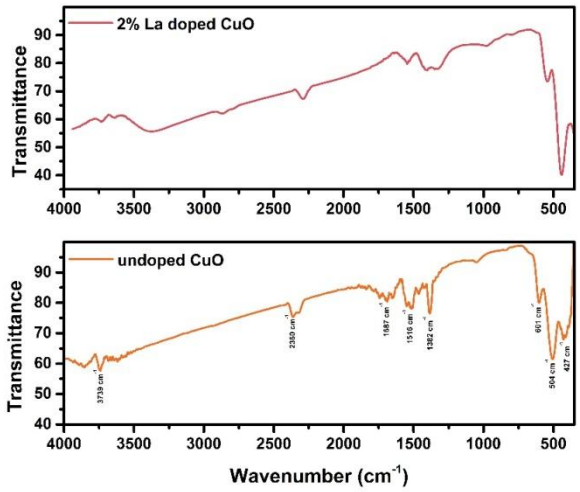

FIGURE 3. FTIR spectra of Pure CuO& 2% La doped CuO NPs

3.3 Optical analysis: UV-Vis-NIR

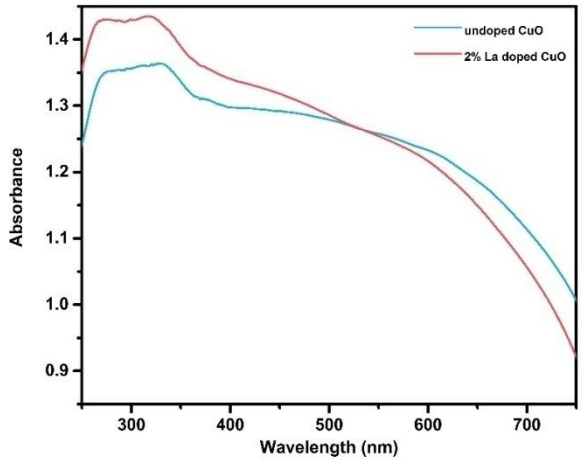

FIGURE 4. UV-Vis spectra of Pure CuO& 2% La doped CuO NPs

The optical analysis of the synthesized CuO and La doped CuO were examined using the UV-Visible absorption spectrophotometer. The samples were recorded in the range of 200-800 nm. In this electromagnetic spectrum the atoms, ions and molecules go through an electronic transition from ground state to the excited state and this defines the amount of absorbed and transmitted light for the given material. Here figure 4 and 5 showcases the optical absorption and the energy structures of Pure CuO and La doped CuO and its corresponding plot of $(\alpha h\nu)^2$ versus $(h\nu)$. The absorption edge of direct inter band changeover is given by [16];

$$\alpha h\nu = C\left(\alpha h\nu - E_g\right)^{1/2} \quad (3)$$

Where, α is the optical absorption co-efficient, hν is the photon energy, E_g is the optical bad gap and C is the constant for a direct transition. The absorption edge [17] for Pure CuO NPs was found to be as 623 nm and likewise for La doped CuO NPs it was found to be as 631 nm. However the energy gap E_g can be found from the intercept of $(\alpha h\nu)^2$ versus $(h\nu)$, where the energy band gap for Pure CuO is found as 2.64 eV and for 2% La doped CuO is found to be as 2.69 eV. From this we can comprehend that the dopant and the doping concentration plays an animated role in the optical property of the nanoparticle.

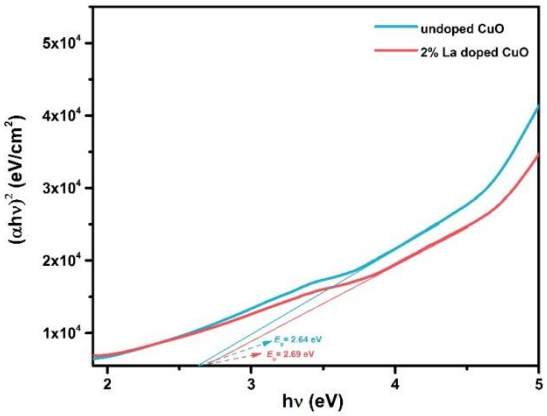

FIGURE 5. Kubelka-Munk Plot of Pure CuO& 2% La doped CuO NPs

3.4 Optical Analysis: Raman Spectra

The CuO is of $C_{2h}^6(C2/c)$ space group, the irreducible demonstrations from the correlation diagram associated with primitive cell's lattice vibrations is given as [18]

$$\Gamma_{RA} = 4A_u + 5B_u + A_g + 2B_g \quad (4)$$

From the 12 vibrations out of which three are Raman acive modes $(A_g + 2B_g)$[19], six are infrared active modes $(3A_u + 3B_u)$ and three are acoustic modes $(A_u + 2B_u)$. Fig.6 shows the raman spectra of undoped and La doped nanoparticles, all the three raman active modes (A_g, B_g^1, B_g^2) were present [20]. There was a negligible red shift seen in the spectrum as the dopant is added, this is due to the phonon confinment effect. At 1196 nm a multiphonon band was recorded apart from the three major raman active modes for both pure and doped samples. This band was formed due to the stretching vibration in the $(x^2 - y^2)$ plane induced by the electronic density variation.

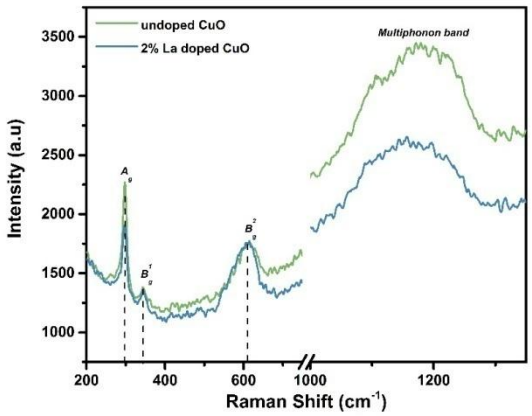

FIGURE 6. Raman Spectra for Pure CuO& 2% La doped CuO NPs

3.5 Morphological analysis: TEM

It can be seen from Table.1 that the crystallite size and lattice parameters increases with the escalation in doping concentration. Figure 7.a&b shows the TEM micrograph of CuO nanoparticles and 2% La doped CuO nanoparticles. It is seen that the Nanoparticles possessed a rod and sheet morphology. The TEM image of Pure CuO and La doped CuO divulges that the powder is agglomerated with polycrystalline NPs [21]. As the doping concentration upsurges, the surface area of the grain decreases and contributes assorted facets.

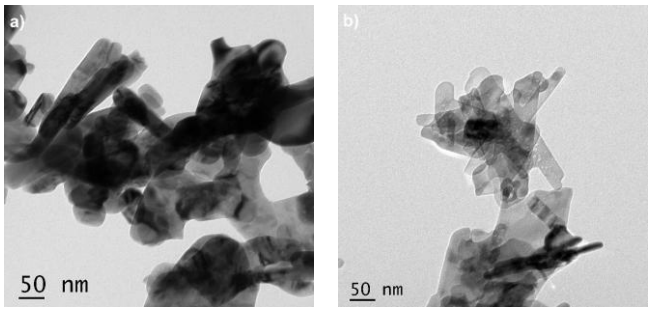

Figure 7.TEM micrograph of a) Pure CuO b) 2% La doped CuO

4 Conclusions

Thus Monoclinic structured CuO and 2% La doped CuO nanoparticles were synthesized by co-precipitation method, resulting in a much reduced crystalline size and beneficial optical properties. The distinctive parameters were calculated from X-ray diffraction which publicized the retention of monoclinic structure and the reduction in the crystallite size. In FTIR spectrum the vibrational band of CuO and the shift in the band due to the addition of the dopant was confirmed. The UV-vis spectrum showed the absorption edge which slightly increases when the dopant is added and the energy band gap was found using Kubelka-Munk plot and it is also found that as the dopant is added there is an increase in the band gap proclaiming an increase in stability of the material, The TEM micrograph gave an elusive idea of evenly distribution of the agglomerated polycrystalline nanoparticles.

Acknowledgements

The authors are grateful to the management of Loyola College, Chennai - 34 for the financial support through the project 3LCTOI14PHY002 under Loyola College TOI-Scheme.

References

[1] B. Sathyaseelan, E. Manikandan, K. Sivakumar, J. Kennedy, and M. Maaza, "Enhanced visible photoluminescent and structural properties of ZnO/KIT-6 nanoporous materials for white light emitting diode (w-LED) application," *J. Alloys Compd.*, vol. 651, pp. 479–482, 2015.

[2] J kennedy, J. Leveneur, G. V Williams, D. R. Mitchell, and A. Markwitz, "Fabrication of surface magnetic nanoclusters using low energy ion implantation and electron beam annealing," *Nanotechnology*, vol. 22, p. 115602, 2011.

[3] C. J. Raj *et al.*, "Two-Dimensional Planar Supercapacitor Based on Zinc Oxide/Manganese Oxide Core/Shell Nano-architecture," *Electrochim. Acta*, vol. 247, pp. 949–957, 2017.

[4] C. N. R. Rao, *Transition-metal oxides*, vol. 6, no. 4. Marcel Dekker, Inc; New York, 1974.

[5] N. M. Mahmoodi and F. Najafi, "Preparation of surface modified zinc oxide nanoparticle with high capacity dye removal ability," *Mater. Res. Bull.*, vol. 47, no. 7, pp. 1800–1809, 2012.

[6] N. Bouazizi, R. Bargougui, A. Oueslati, and R. Benslama, "Effect of synthesis time on structural, optical and electrical properties of CuO nanoparticles synthesized by reflux condensation method," *Adv. Mater. Lett.*, vol. 6, no. 2, pp. 158–164, 2015.

[7] J. D. Rodney *et al.*, "Photo-Fenton degradation of nano-structured La doped CuO nanoparticles synthesized by combustion technique," *Optik (Stuttg).*, 2018.

[8] P. Annie Vinosha, B. Xavier, A. Ashwini, L. Ansel Mely, and S. Jerome Das, "Tailoring the photo-Fenton activity of nickel ferrite nanoparticles synthesized by low-temperature coprecipitation technique," *Optik (Stuttg).*, vol. 137, pp. 244–253, 2017.

[9] S. J. Priscilla *et al.*, "Structural and Morphological properties of Lithium Doped Copper Oxide Nanoparticles," *Int. J. Mater. Sci.*, vol. 12, no. 2, pp. 245–249, 2017.

[10] P. Scherrer, "Bestimmung der Größe und der inneren Struktur von Kolloidteilchen mittels Röntgenstrahlen," *Math. Klasse*, vol. 29, pp. 98–100, 1918.

[11] A. L. Patterson, "The scherrer formula for X-ray particle size determination," *Phys. Rev.*, vol. 56, no. 10, pp. 978–982, 1939.

[12] A. Sahai and N. Goswami, "Structural and vibrational properties of ZnO nanoparticles

synthesized by the chemical precipitation method," *Phys. E Low-Dimensional Syst. Nanostructures*, vol. 58, pp. 130–137, 2014.

[13] F. Fang, J. Kennedy, D. Carder, J. Futter, and S. Rubanov, "Investigations of near infrared reflective behaviour of TiO2 nanopowders synthesized by arc discharge," *Opt. Mater. (Amst).*, vol. 36, no. 7, pp. 1260–1265, 2014.

[14] R. E. Rundle, Kazuo Nakamoto, and M. Margoshes, "Stretching Frequencies as a Function of Distances in Hydrogen Bonds," *J. Am. Chem. Soc.*, vol. 77, pp. 6480–6486, 1955.

[15] G. Busca, "FT-IR study of the surface of copper oxide," *J. Mol. Catal.*, vol. 43, pp. 225–236, 1987.

[16] Y. Li, J. Huang, L. Cao, J. Wu, and J. Fei, "Optical properties of La2CuO4 and La2−xCaxCuO4 crystallites in UV–vis–NIR region synthesized by sol–gel process," *Mater. Charact.*, vol. 64, pp. 36–42, 2012.

[17] Q. Chen and D. Ma, "Preparation of Nanostructured Cu 2 SnS 3 Photocatalysts by Solvothermal Method," *Int. J. Photo*, vol. 2013, pp. 3–7, 2013.

[18] M. A. Dar, Q. Ahsanulhaq, Y. S. Kim, J. M. Sohn, W. B. Kim, and H. S. Shin, "Versatile synthesis of rectangular shaped nanobat-like CuO nanostructures by hydrothermal method; structural properties and growth mechanism," *Appl. Surf. Sci.*, vol. 255, no. 12, pp. 6279–6284, 2009.

[19] T. H. Tran and V. T. Nguyen, "Copper Oxide Nanomaterials Prepared by Solution Methods, Some Properties, and Potential Applications: A Brief Review," *Int. Sch. Res. Not.*, vol. 2014, pp. 1–14, 2014.

[20] S. Guha, D. Peebles, and J. Wieting, "Raman and infrared studies of cupric oxide," *Bull. Mater. Sci.*, vol. 14, no. 3, p. 539, 1991.

[21] R. Kam, C. Selomulya, R. Amal, and J. Scott, "The influence of La-doping on the activity and stability of Cu/ZnO catalyst for the low-temperature water-gas shift reaction," *J. Catal.*, vol. 273, no. 1, pp. 73–81, 2010.